

NICMOS Status and Plans

Rodger I. Thompson

Steward Observatory, University of Arizona, Tucson, AZ 85721

Abstract. NICMOS has been in orbit for about 8 months. This is a report on its current status and future plans. Also included are some comments on particular aspects of data analysis concerning dark subtraction, shading, and removal of cosmic rays.

1. Introduction

Since the beginning of NICMOS operation in February of 1997 there have been several thousands of images taken. Most of these have been related to the Servicing Mission Observatory Verification (SMOV) program and calibration observations, however, recently many GO science programs have executed. The following is a summary of the current status of NICMOS and some future plans. This paper does not extensively cover the coronagraphic and polarimetric aspects as there are other presentations in this conference on those issues. Some aspects of data reduction are covered to help the users of NICMOS obtain the best scientific benefit from their observations.

2. Current Status

At present NICMOS provides excellent images of high scientific content. Most of the observations utilize Cameras 1 and 2 which are in excellent focus. Camera 3 is not yet within the range of the focus adjustment mechanism, but its current images are still quite excellent. In the following we will present the status of various aspects of the NICMOS instrument.

2.1. Photometric Status

All three of the NICMOS cameras are operational and capable of delivering excellent photometric images. The photometric characteristics of the cameras are well within the original design specifications and are close to the expected performance maximums predicted before launch. The primary photometric characteristics are shown in Table 1 below:

Table 1. Photometric Characteristics

Camera	Noise ^a	Dark Current ^b	Gains ^c
1	22	0.16	5.4
2	29	0.15	5.4
3	30	0.15	6.5

^aValue in electrons

^bValue in electrons per second

^cValue in electrons per ADU

Background Flux The NICMOS background fluxes are dominated by the natural zodiacal light background at wavelengths shorter than 2 microns and by the thermal emission from the HST mirrors at longer wavelengths. The overall background is about two thirds of the flux expected from Instrument Design Team's (IDT) calculations and significantly less than the early handbook listings. This is partially due to a lower operating temperature of the main HST optics than assumed in the calculations. The zodiacal background estimates were also on the conservative side.

2.2. Photometric Calibration

During SMOV there were observations of two photometric standard stars in a few selected filters. These results are shown in Table 2. The Camera 3 data were taken with the Field Offset Mirror (FOM) in a position that created vignetting in Camera 3. The vignetting created a high thermal background so no background numbers are quoted for Camera 3.

Table 2. Photometric Response

Camera	Filter	e/sec per Jy	background	Flux for S/N = 1 ^a
1	F090M	3.72×10^5	0.10	1.83×10^{-7}
1	F110M	7.10×10^5	0.11	9.51×10^{-8}
1	F145M	9.25×10^5	0.13	7.00×10^{-8}
1	F165M	1.12×10^6	0.20	5.93×10^{-8}
2	F110W	2.37×10^6	0.30	3.62×10^{-8}
2	F165M	1.16×10^6	0.26	7.39×10^{-8}
2	F207M	8.49×10^5	0.59	2.29×10^{-7}
2	F222M	8.93×10^5	9.00	3.91×10^{-7}
2	F237M	1.12×10^6	39.0	6.26×10^{-7}
3	F110W	2.12×10^6		3.33×10^{-8}
3	F160W	2.17×10^6		3.64×10^{-8}
3	F166N	9.76×10^4		5.45×10^{-7}
3	F222M	9.00×10^5		7.76×10^{-7}
3	F240M	1.47×10^6		1.41×10^{-6}

^aSignal in Jy for 1000 second integration

2.3. Optical Status

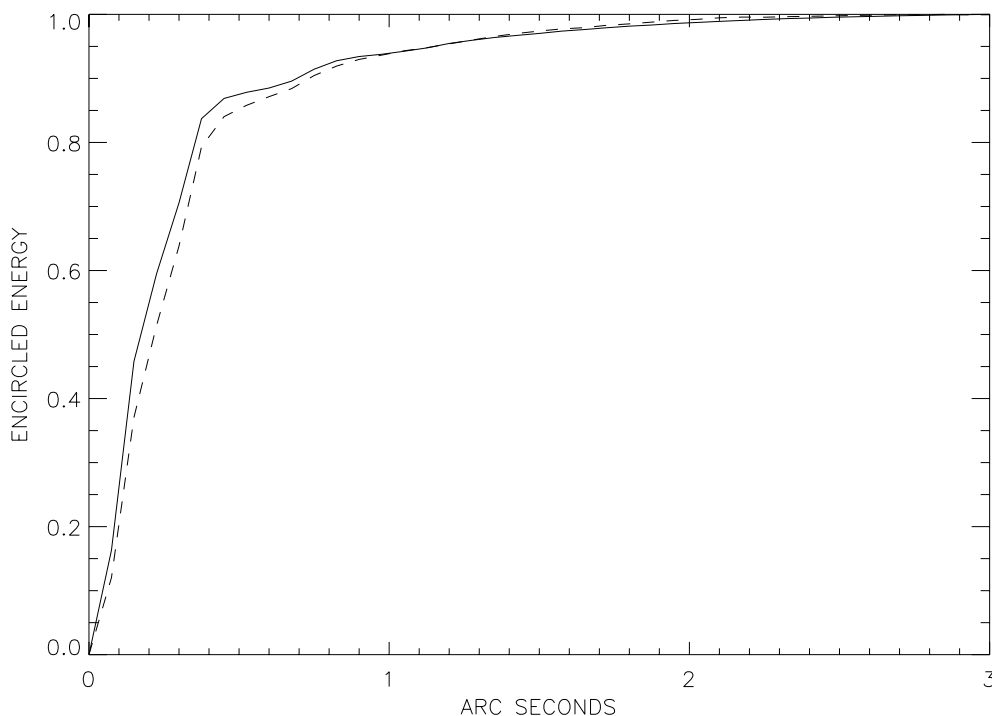
NICMOS Cameras 1 and 2 have excellent images that meet all of the Point Spread Function (PSF) and encircled energy specifications. Sharply defined Airy rings are evident in all images. The depth of focus range for these cameras overlap and there is a common focus position specified for these cameras.

Camera 3 has a focus position that is currently beyond the range of the focus adjustment mechanism, however, the current images are of high quality and quite sufficient for many investigations. This is a great improvement over the image data taken early in the mission.

Camera 1 and 2 Image Quality Our most utilized camera has been Camera 2 followed by Camera 1. Figure 1 has a comparison of the encircled energy of an actual Camera 2 image with a synthetic image from the TinyTim PSF synthesis package. The solid line is the theoretical image and the dashed line is the measured encircled energy. The measurement is for an isolated star in the F160W filter.

Camera 3 Image Quality At the present time the energy contained in the central pixel of a Camera 3 PSF is about 65 percent of the theoretical maximum. This is an excellent image quality for many programs and represents a significant improvement over the image quality near the beginning of the mission. The rate of focus return has declined in the last

Figure 1. The solid line is the theoretical, the dashed line is the measured encircled energy distribution



few months but continues to be in the desired direction. We expect further improvement during the course of the mission but quantitative predictions are not warranted.

Observations with the current FOM setting for Camera 3 yield a vignetted image. Recent FOM offset observations indicated that the vignetting is eliminated for an offset FOM setting. A new default Camera 3 FOM setting is under development at STScI.

Plate Scales and Apertures At the present time the following are the best representations of the plate scales and apertures for the three NICMOS cameras. As the focus moves further back the numbers for Camera 3 may need alteration. The plate scales are in arc seconds per pixel and the aperture reference angle is in degrees from the +V3 axis in the SIAF frame. The image plane of NICMOS is slightly tilted at the detector arrays. This tilt creates the difference between the X and Y plate scales.

Table 3. The NICMOS Plate Scales

Camera	X-scale	Y-scale	X-FOV	Y-FOV	V3 Angle
1	0.043328	0.043231	11.09190	11.04154	315.3270
2	0.076216	0.075502	19.52282	19.32851	314.5190
3	0.204538	0.203916	52.36173	52.20250	314.8610

NICMOS currently supports two standard aperture positions in addition to the special apertures associated with coronagraphic images. The NICMOS FIX apertures are at the center of the detector array at the intersection of row and column 127 (0 is the first row or column). The straight NICMOS apertures are given below.

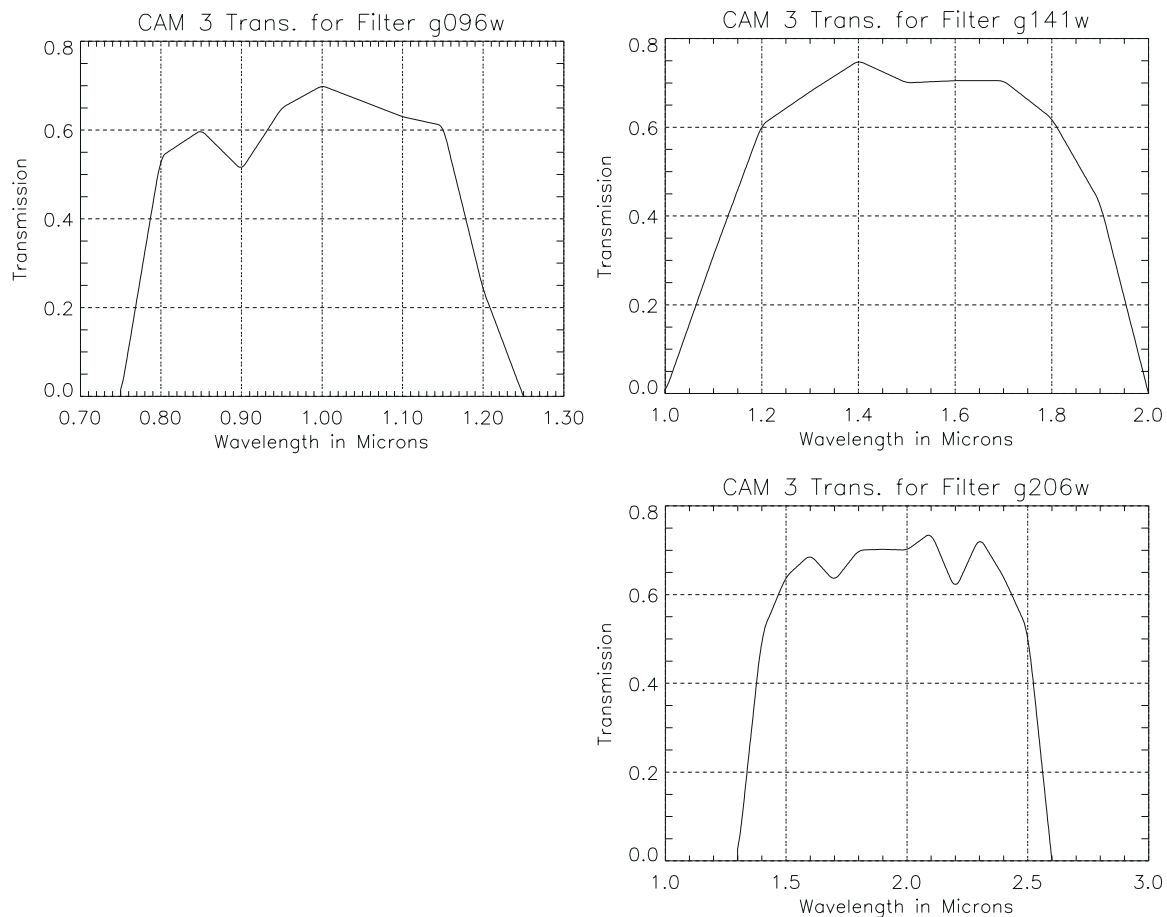
Table 4. NICMOS Aperture Locations

Camera	X-pixel	Y-pixel
1	162	100
2	149	160
3	140	135

2.4. Spectroscopic Status

NICMOS contains three gratings in Camera 3, G096, G141, and G206 with resolutions of $R=200$ per pixel or $R=100$ for Nyquist sampling. These gratings cover the full wavelength range of NICMOS. G096 and G141 have wavelength ranges with minimal background contamination. G206, however, receives substantial thermal background radiation from the HST optics. At this point we do not have a wavelength calibration for the gratings. Inspection of the parallel grating observations indicates that the gratings appear to be operating as designed. Figure 2 indicates the grating efficiency functions.

Figure 2. These are the efficiency curves for the gratings measured during ground testing of the grating optics only.



2.5. Polarization and Coronagraphic Status

These areas are covered in other articles in this volume so only summary remarks will occur here. Polarization studies have been carried out with the NICMOS polarizers. Their lower than expected polarization efficiency and non-symmetrical angles require a different computational algorithm than appears in the NICMOS Instrument Handbook (MacKenty et al., 1997). Refer to the article in this volume on polarization (Hines, Schmidt & Lytle 1997). With the modified computational procedures polarizations on the order of a few percent can be measured. The NICMOS polarizers are intended for highly polarized objects such as star formation regions.

Coronagraphic tests were performed during the SMOV and calibration observations. These tests showed that coronagraphic observations at two different roll angles reduce the scattered light by about a factor of 30 over non-coronagraphic imaging. Refer to the article on NICMOS coronagraphic observations (Schneider) At spacings greater than the radius of the occulting spot ($0''.3$) coronagraphic imaging is very effective in detecting faint objects or structure near bright objects.

It should also be noted that NICMOS has a very low-scattering optical train. This, coupled with very low cross talk and no charge transfer makes the detection of faint structures in the presence of bright objects reasonably easy even without the coronagraph. The combination of these characteristics with the coronagraph makes NICMOS a very powerful tool for planet or brown dwarf detection as well as the study of structure around bright quasars.

3. Future Plans

The Space Telescope Science Institute has committed itself to utilizing NICMOS efficiently until the end of its cryogenic lifetime. The Call for a delta round of proposals was part of that commitment. STScI is also committed to at least two Camera 3 imaging campaigns which put the camera in focus by a small adjustment of the HST secondary. The first campaign is scheduled for late this year and the second will occur next year unless the camera returns to proper focus on its own.

The same motion that produced the focus anomaly also produced the thermal contact that is limiting the lifetime of the instrument. It is not known if this thermal contact will release in the future. If it does not the cryogen will last until approximately February of 1999. If the thermal contact does release the lifetime will depend upon the time of release. Goddard Space Flight Center is studying the possibility of installing an auxiliary cryogenic cooler for NICMOS during the 1999 HST Maintenance Mission. If this mechanism is successful the lifetime of NICMOS could be extended indefinitely.

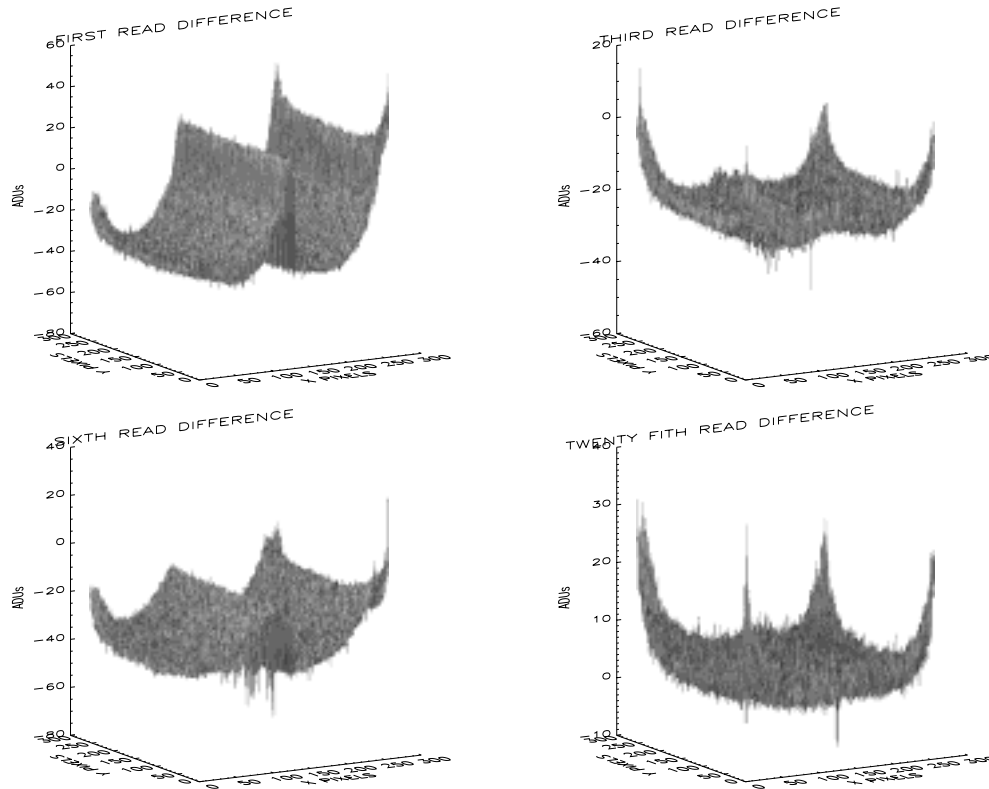
4. Some Aspects of Data Analysis

The NICMOS IDT has pursued some aspects of data analysis and reduction in parallel to the efforts of STScI and the pipeline analysis procedures. One of these alternative procedures follows the flow listed here.

1. Start with the raw fits data
2. Form the first differences ($\text{Read1} - \text{Read0}$, $\text{Read2} - \text{Read1}$, etc)
3. Subtract the cosmic ray cleaned darks of the same sampling sequence. Make sure the proper history has been kept on the dark frames.
4. Perform the linearity correction

5. Perform the cosmic ray elimination.
6. Perform the flat field correction

Figure 3. Dark first differences showing shading



4.1. Comments on Data Analysis

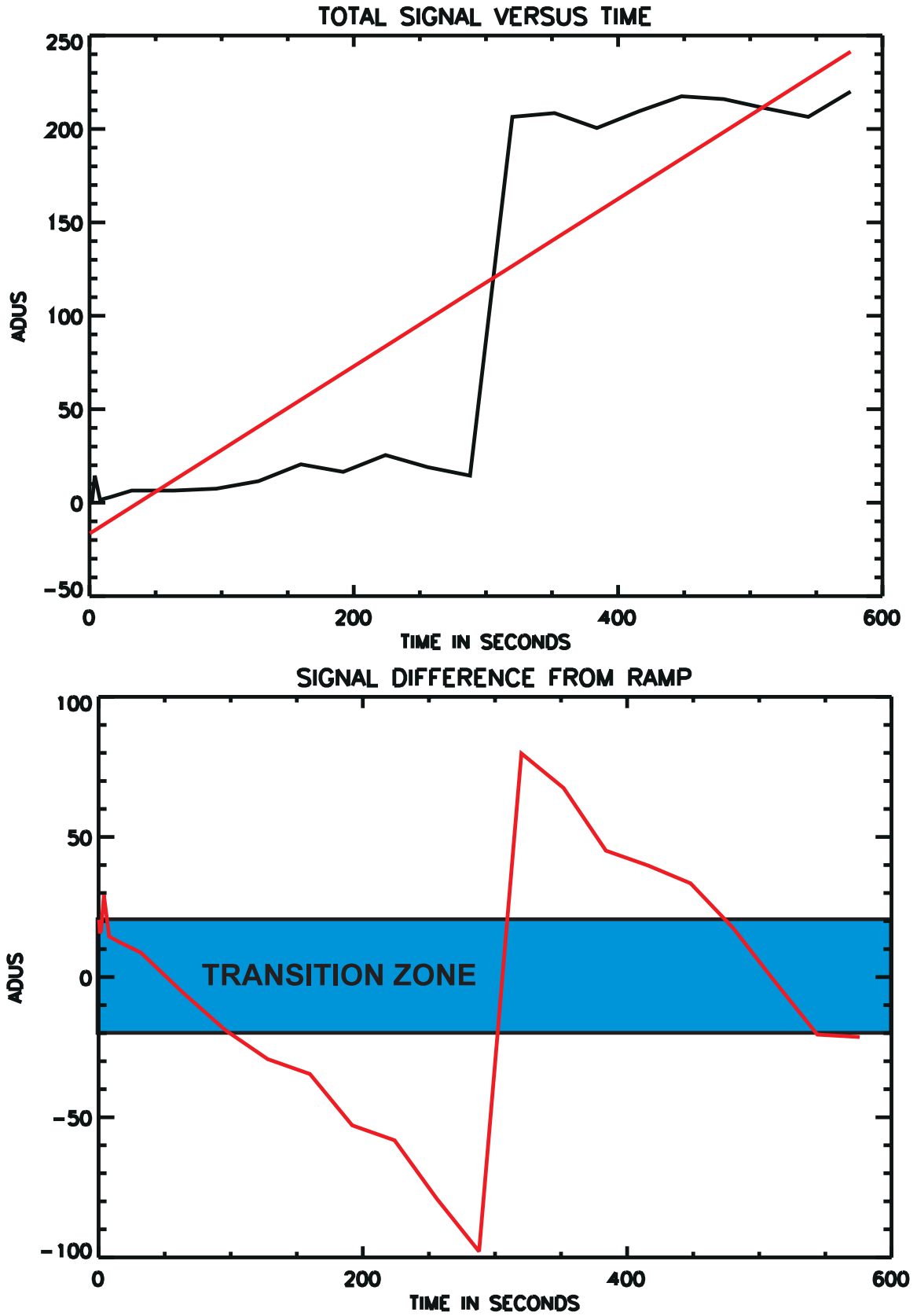
In this last section are some comments on a few aspects of the data analysis procedure shown above that may help some observers.

First Differences This analysis uses the first differences as the fundamental data unit. Each of the first differences in a multi-accum integration contains independent signal data. This is very useful in a statistical evaluation of the signal. Also, first differences that are contaminated in any way can be discarded and not affect the flow of the data analysis.

Dark Subtraction In subtracting the dark frames it is important to know the history of the dark frames and the image frames. Darks and images are frequently taken in substantial blocks with no pause between them. The initial observations with NICMOS showed what is now termed the pedestal effect. The first and second multi-accum observations differed from later ones by having an excess flux levels on the order of a few tens of ADUs per pixel for the whole integration and an altered shading structure. This was most apparent in the 127 column of Cameras 2 and 3 and the 127 row of Camera 1.

Particular care should be taken to subtract the first dark integration of a sequence from the first image of a sequence and the second dark from the second image. After two images

Figure 4. Relevant signals for cosmic ray elimination.



a median dark of the remaining darks in the sequence can be subtracted from the remaining images. If the images are part of a dither pattern the small delay may partially reset the effect and an appropriate combination of first and second darks may be more appropriate.

Figure 3 shows the shading characteristics of a darkframe for the first third sixth and last first difference in Camera 2. Note the very sharp discontinuity at column 127 in the first of the first differences and again for the sixth. It is slight changes in the depth of this discontinuity that causes a stripe in column 127 if there has not been proper history kept in the dark frames.

There has been a flight software change in an attempt to eliminate the pedestal effect. The NICMOS detectors are in a state of constant readout when they are not in use. The flight software now maintains the detector output amplifiers in an ON state during this time. It is hoped that this will stabilize the amplifiers during integration. The effectiveness of these changes is under evaluation.

Cosmic Ray Elimination The non-destructive readout mode of the NICMOS detectors offers a very efficient mechanism for detecting and eliminating cosmic ray hits. The mechanism also allows collection of useful information after the cosmic ray hit as long as the pixel is not saturated.

The various multi-accum sample sequences record the signal levels at several times during the integration. This provides a history of the signal in any pixel as a function of time. Cosmic ray hits produce an instantaneous step in the signal level. Cosmic rays are detected by searching for this signature.

One of the cosmic ray elimination packages developed by the team fits the signal versus time function with a linear function. The fit is very poor at the step function caused by the cosmic ray. The difference between the fit and the actual signal shows a very sharp negative to positive transition at the cosmic ray event.

The program looks for this signature in both the difference function and the ratio of the difference to the actual signal. It also utilizes the variance of the fit as another indicator of a true hit. Once a cosmic ray has been identified the bad first difference is removed and a new fit performed. The value predicted by the new fit replaces the bad first difference. In this way all signals other than the bad read are utilized. The linearity correction performed earlier in the process identifies and flags saturated cosmic ray hits.

Acknowledgments. The NICMOS team wishes to thank the dedicated personnel at Ball Aerospace, Rockwell International, NASA Goddard Space Flight Center, NASA Headquarters, and the Space Telescope Science Institute who have worked over the last 13 years to make this mission possible. We also greatly thank the crew of STS 82 who installed NICMOS into HST along with STIS and greatly improved the overall performance of the telescope. NICMOS was built under NASA contract NASA 5-31289 and this work is supported in part by NASA grant NAG 5-3042. This article is based in part on observations with the NASA/ESA Hubble Space Telescope, obtained at the Space Telescope Science Institute, which is operated by the Association of Universities for Research in Astronomy under NASA contract NAS5-26555.

References

Mackenty, J. W., et al., 1997, *NICMOS Instrument Handbook*, Version 2.0 (Baltimore: STScI).